
A COMPARATIVE ANALYSIS OF DEEP LEARNING MODELS FOR LUNG SEGMENTATION ON X-RAY IMAGES

• Weronika Hryniewska-Guzik, Jakub Bilski*

Bartosz Chrostowski*, Jakub Drak Sbahi*, • Przemysław Biecek

Faculty of Mathematics and Information Science
Warsaw University of Technology, Poland
weronika.hryniewska.dokt@pw.edu.pl

ABSTRACT

Robust and highly accurate lung segmentation in X-rays is crucial in medical imaging. This study evaluates deep learning solutions for this task, ranking existing methods and analyzing their performance under diverse image modifications. Out of 61 analyzed papers, only nine offered implementation or pre-trained models, enabling assessment of three prominent methods: Lung VAE, TransResUNet, and CE-Net. The analysis revealed that CE-Net performs best, demonstrating the highest values in dice similarity coefficient and intersection over union metric.

Keywords Semantic segmentation, X-ray, Lungs, Deep Learning, U-Net

1 Introduction

In the field of medical imaging, accurate segmentation of lungs on X-rays is important in many applications [6], from early disease detection to treatment planning and patient monitoring. As healthcare evolves, the need for fast and accurate tools grows, implying physician support with deep learning approaches [5]. In particular, solutions such as U-Net demonstrate the potential to automate the task of lung segmentation, offering promising advances in improved accuracy [8].

However, despite these advances, the inevitable diversity of X-ray images makes it difficult for some modern segmentation methods to deal with them. Although many solutions show high performance in simple and typical cases, their performance degrades when confronted with complex ones. Moreover, the issue of using pre-trained models on images with different characteristics may have potential negative consequences when used for real-world solutions [3].

Recognizing these challenges, our objective is to analyze existing solutions for lung segmentation and systematically evaluate their performance across a dataset of varying characteristics. In this study, we analyze and compare three prominent methods - Lung VAE, TransResUNet, and CE-Net - using five image modifications. The ultimate goal is to determine the most accurate method for lung segmentation in diverse scenarios.

2 Methodology

The complexity of the lung segmentation task is related to the scarcity of actual data containing X-ray images and its masks with diverse obstructions such as jewelry, advanced stages of disease, and some medical devices present in a patient's body. To address this limitation, we merged two existing datasets: Montgomery County X-ray [1] and Shenzhen Hospital X-ray [4]. The first one contains 138 X-rays, of which 80 are normal and 58 are abnormal with

*equal contribution

manifestations of tuberculosis. Alongside the lung, segmentation is provided. The second one contains 340 normal and 275 abnormal X-rays showing various manifestations of tuberculosis. The masks are provided by Stirenko et al. [11].

For our analysis of models dedicated for lung field segmentation, we select 54 methods documented in Çalli et al. [12] and seven scientific papers which implementation is available on Github platform models. Most of the solutions could not be run due to obsolete versions of libraries, lack of the reproduction steps in the article/repository, not working parts of code, and lack of methods for using data other than those provided with code. Finally, we are able to run only three of them, described in Section 3.

If there was a pre-trained model available for any of the architectures, it was used for the evaluation process. Otherwise, a model was trained on the data on which it was originally trained, as it was described in the source article.

Then, an evaluation was performed on the prepared test data. It contained both original and augmented images. For every pair of ground-true and predicted mask, the quality of segmentation was assessed using dice similarity coefficient [10] and intersection over union (IoU). The following augmentations, presented in Figure 1, were done: contrast, random rotation, bias field, horizontal flip, and discrete "ghost" artifacts. The resulting dataset allowed us to perform testing on model behavior when presented with an image with augmentation that was not present in the training phase.

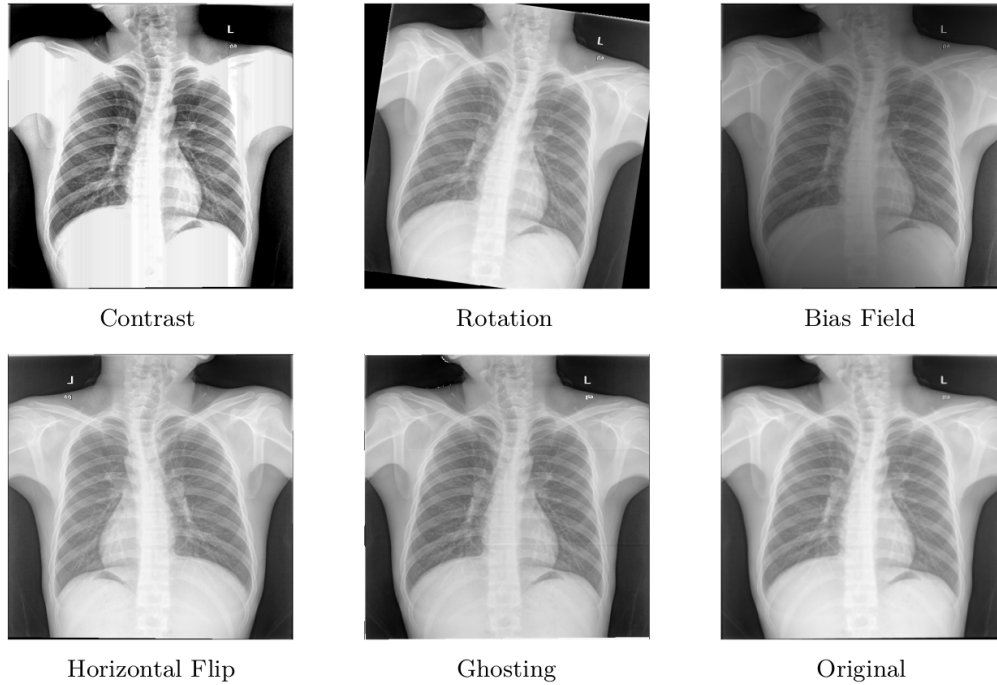


Figure 1: Types of augmentation on which the ability to adapt to new conditions of segmentation models was tested.

3 Related Works

Lung VAE [9]^b aim is to be a lung segmentation model that is not dependent on training set distribution. For this purpose, a U-net-based segmentation network encoder and variational encoder is used. As the authors did not train the model on opacity cases, the variational encoder is used for data imputation and may be treated as data augmentation. The results of U-net encoder and variational encoder are concatenated and passed to the decoder.

TransResUNet [7]^c is an improved version of U-net [8] model dedicated for the task of lung field segmentation. Three modifications were made. First, a pre-trained encoder was taken from VGG-16 architecture trained on the ImageNet dataset. The first seven layers were used. As a second improvement, between the encoder and decoder layers were added skip connections with a series of convolution blocks. Finally, a dedicated post-processing step with hole filling, artefacts removal and morphological opening was applied to the output images.

^b<https://github.com/raghavian/lungVAE>

^c<https://github.com/sakibreza/TransResUNet>

CE-Net [2]^d is a U-net-based approach of a context encoder network. Its aim is to capture more abstract and preserve spatial information for 2D medical image segmentation. There are three components: a feature encoder module, a context extractor, and a feature decoder module. For feature extraction, pretrained ResNet-34 is used. Dense atrous convolution block and residual multi-kernel pooling are used for context extraction. In feature decoder module, transposed convolution is applied.

4 Results and discussion

The Lung VAE model, shown in Figure 2a, obtained the best results for images without augmentations and the worst for the Random Bias Field augmentation. From the augmented images, it seems to have the best results for the Random Ghosting.

Figure 2b illustrates the results for the TransResUNet model, which performed less favorably compared to the other two methods. The mean dice loss for images without augmentation was slightly greater than 80%. Three augmentation types had no real effect on the results; Random Affine, Random Flip, and Random Ghosting achieved a very similar mean dice loss as the case with no augmentation. The two remaining augmentation methods posed a more serious problem. Contrast got a slightly lower dice loss and a thicker tail of the distribution, while Random Bias Field performed much worse, with a very long tail and low mean score. While other methods also struggled with this type of augmentation, this method seemed to perform the worst.

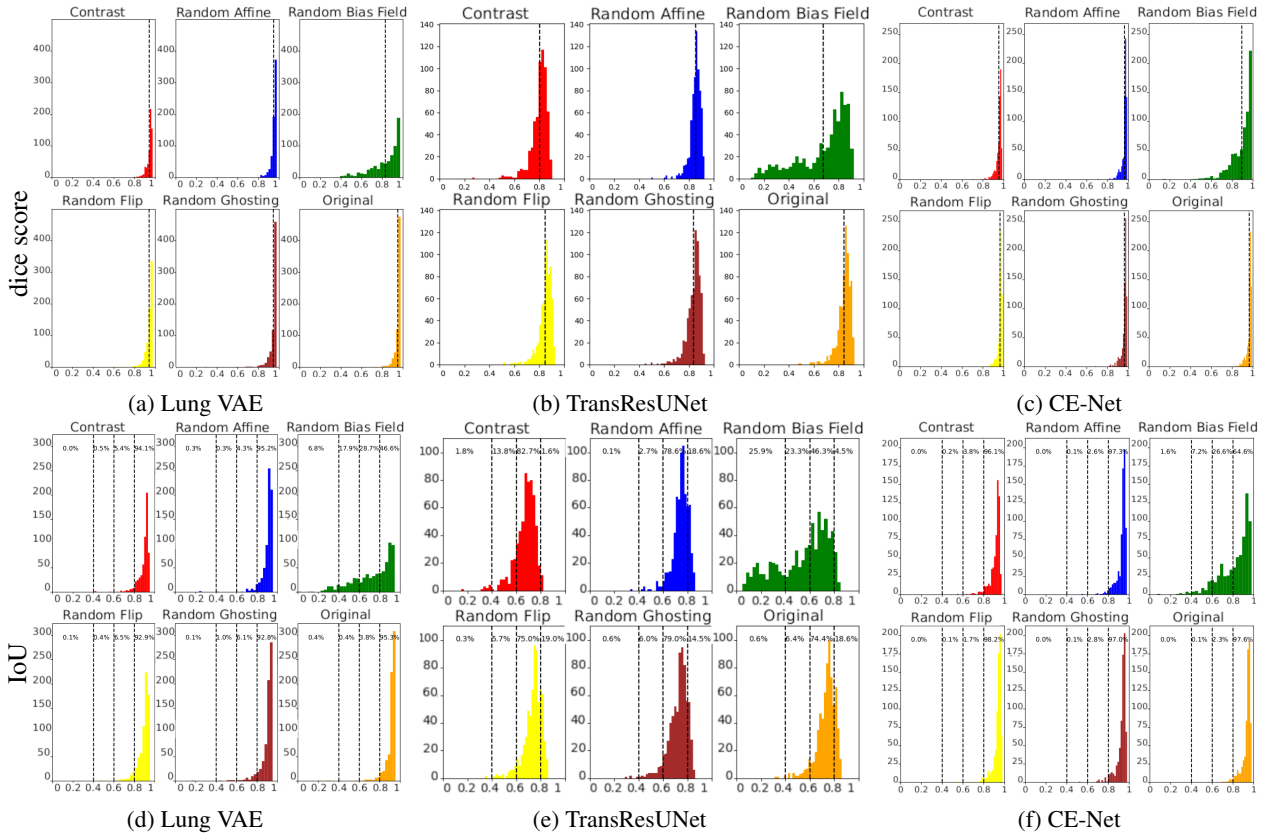


Figure 2: Segmentation results (dice similarity coefficient and IoU value) after applying various augmentation methods that have not been performed on the training set before. On the horizontal axis is the dice similarity coefficient value from 0 to 1, and on the vertical axis is the number of samples from 0 to 500.

The results for CE-Net are presented in Figure 2c, showcasing its outperformance relative to both Lung VAE and TransResUNet. This distinction is particularly noticeable for the Random Bias Field augmentation, where CE-Net exhibited a better average dice similarity coefficient and a significantly shorter low-tail compared to the other two models.

^d<https://github.com/Guzaiwang/CE-Net>

Figure 2d, 2e, and 2f illustrate the results for the IoU score, providing a summary of the score distribution. Here, the robustness of CE-Net is evident, with very few samples falling outside the best score bin. In contrast, TransResUNet displayed a thicker tail, with some samples consistently reaching the worst bin and a peak in the third bin. Although Lung VAE performed slightly worse than CE-Net in all cases, it still achieved significantly better results than TransResUNet, emphasizing CE-Net as the superior and more reliable algorithm.

Figure 3 shows an example of the segmentation results of the original image for three models using different previously unseen augmentations. As was presented in the aggregated analysis, the CE-Net model in all augmentations managed to obtain satisfying results. The most significant differences between outputs of CE-Net and Lung VAE are visible in Figure 3b. The Lung VAE model captured the position of the lung. However, the obtained mask did not manage to preserve the shape, especially in the top part of the image. TransResUNet often detects spots outside of the lung that seem to correspond with places with a darker shade of gray than the rest of the body.

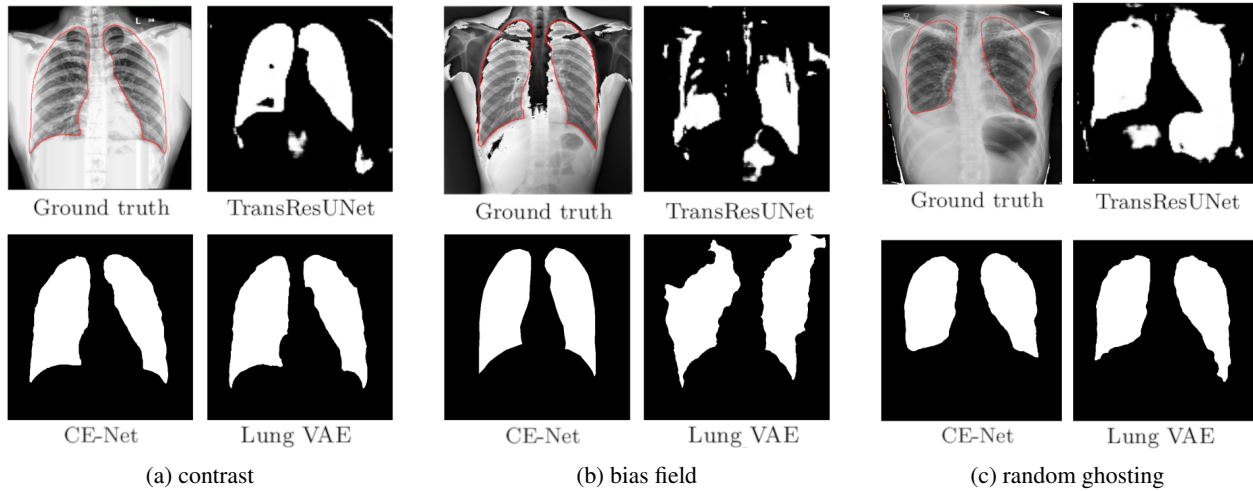


Figure 3: Original X-ray images with segmented lungs (marked in red) compared to lung masks generated by various models using different augmentation methods.

5 Conclusions

In literature, the vast majority of solutions for lung segmentation are based on the U-net architecture enhanced with either the preprocessing of data or the post-processing of output masks. It is worth stressing that when proposing a new architecture, it is necessary to ensure that the results are reproducible. Among the 61 examined papers, only three demonstrated effective solutions: CE-Net, TransResUNet, and Lung VAE.

Evaluation of these lung segmentation methods based on dice loss and IoU metrics revealed consistent superiority of CE-Net across experiments. Notably, TransResUNet exhibited limitations, struggling to accurately localize the lungs in certain instances. The direct comparison of generated masks further emphasized the robust performance of CE-Net over both TransResUNet and Lung VAE.

These findings highlight the challenges in achieving reliable and consistent results in deep learning for segmentation tasks, underscoring the significance of methodological choices in model development. The code is available at <https://github.com/Hryniewska/lung-segmentation-on-X-rays>.

Acknowledgment

The authors would like to thank Jakub Brojacz for his valuable impact on the research.

References

- [1] S. Candemir, S. Jaeger, K. Palaniappan, J. P. Musco, R. K. Singh, Z. Xue, A. Karargyris, S. Antani, G. Thoma, and C. J. McDonald. Lung segmentation in chest radiographs using anatomical atlases with nonrigid registration. *IEEE Transactions on Medical Imaging*, 33(2):577–590, 2014. doi:10.1109/TMI.2013.2290491.
- [2] Z. Gu, J. Cheng, H. Fu, K. Zhou, H. Hao, Y. Zhao, T. Zhang, S. Gao, and J. Liu. CE-Net: Context Encoder Network for 2D Medical Image Segmentation. *IEEE Transactions on Medical Imaging*, 38(10):2281–2292, 2019. doi:10.1109/TMI.2019.2903562.
- [3] S. Hinterstoisser, V. Lepetit, P. Wohlhart, and K. Konolige. On pre-trained image features and synthetic images for deep learning. In *Proceedings of the European Conference on Computer Vision (ECCV) Workshops*, September 2018.
- [4] S. Jaeger, A. Karargyris, S. Candemir, L. Folio, J. Siegelman, F. Callaghan, Z. Xue, K. Palaniappan, R. K. Singh, S. Antani, G. Thoma, Y.-X. Wang, P.-X. Lu, and C. J. McDonald. Automatic tuberculosis screening using chest radiographs. *IEEE Transactions on Medical Imaging*, 33(2):233–245, 2014. doi:10.1109/TMI.2013.2284099.
- [5] W. Liu, J. Luo, and e. a. Yang, Yu. Automatic lung segmentation in chest x-ray images using improved u-net. *Scientific Reports*, 12:8649, 2022. doi:10.1038/s41598-022-12743-y.
- [6] N. Reamaroon, M. W. Sjoding, and e. a. Derksen, Hanneke. Robust segmentation of lung in chest x-ray: Applications in analysis of acute respiratory distress syndrome. *BMC Medical Imaging*, 20(1):116, 2020. doi:10.1186/s12880-020-00514-y.
- [7] S. Reza, O. B. Amin, and M. Hashem. TransResUNet: Improving U-Net Architecture for Robust Lungs Segmentation in Chest X-rays. In *TENSYMP*, pages 1592–1595, 2020. doi:10.1109/TENSYMP50017.2020.9230835.
- [8] O. Ronneberger, P. Fischer, and T. Brox. U-Net: Convolutional networks for biomedical image segmentation. In N. Navab, J. Hornegger, W. M. Wells, and A. F. Frangi, editors, *MICCAI*, pages 234–241, 2015. doi:10.1007/978-3-319-24574-4_28.
- [9] R. Selvan, E. B. Dam, N. S. Detlefsen, S. Rischel, K. Sheng, M. Nielsen, and A. Pai. Lung segmentation from chest X-rays using variational data imputation. *Artemiss workshop at ICML*, 2020.
- [10] R. R. Shamir, Y. Duchin, J. Kim, G. Sapiro, and N. Harel. Continuous dice coefficient: a method for evaluating probabilistic segmentations. *arxiv*, 2019.
- [11] S. Stirenko, Y. Kochura, O. Alienin, O. Rokovyi, Y. Gordienko, P. Gang, and W. Zeng. Chest X-Ray analysis of tuberculosis by deep learning with segmentation and augmentation. In *IEEE ELNANO*, Apr. 2018. doi:10.1109/elnano.2018.8477564.
- [12] E. Çallı, E. Sogancioglu, B. van Ginneken, K. G. van Leeuwen, and K. Murphy. Deep learning for chest X-ray analysis: A survey. *Medical Image Analysis*, 72:102125, 2021. doi:10.1016/j.media.2021.102125.